Inorganic Chemistry

Article

pubs.acs.org/IC

Structural Diversity, Optical and Magnetic Properties of a Series of Manganese Thioarsenates with 1,10-Phenanthroline or 2,2′-Bipyridine Ligands: Using Monodentate Methylamine as an Alkalinity Regulator

Guang-Ning Liu, Guo-Cong Guo,* Feng Chen, Shuai-Hua Wang, Jing Sun, and Jin-Shun Huang

State Key Laboratory of Structural Chemistry, Fujian Institute of Research on the Structure of Matter, Chinese Academy of Sciences, Fuzhou, Fujian 350002, P. R. China

Supporting Information

ABSTRACT: The exploration in two hydro(solvo)thermal reaction systems As/S/Mn^{2+}/phen/methylamine aqueous solution and As/S/Mn^{2+}/2,2′-bipy/H_2O affords five new manganese thioarsenates with diverse structures, namely, $(CH_3NH_3)\{[Mn(phen)_2](As^VS_4)\}\cdot$phen (**1** and **1′**), $(CH_3NH_3)_2\{[Mn(phen)]_2(As^VS_4)_2\}$ (**2**), $\{[Mn(phen)_2](As^{III}_2S_4)\}_n$ (**3**), $\{[Mn(phen)]_3(As^{III}S_3)_2\}\cdot H_2O$ (**4**), and $\{[Mn(2,2'\text{-bipy})_2]_2(As^VS_4)\}[As^{III}S(S_5)]$ (**5**). Compound **1** comprises a $\{[Mn(phen)_2](As^VS_4)\}^-$ complex anion, a monoprotonated methylamine cation and a phen molecule. Compound **2** contains a butterfly like $\{[Mn(phen)]_2(As^VS_4)_2\}^{2-}$ anion charge compensated by two monoprotonated methylamine cations. Compound **3** is a neutral chain formed by a helical $^1{}_\infty(As^{III}S_2^-)$ *vierer* chain covalently bonds to $[Mn^{II}(phen)]^{2+}$ complexes via all its terminal S atoms. Compound **4** features a neutral chain showing the stabilization of noncondensed $(As^{III}S_3)^{3-}$ anions in the coordination of $[Mn^{II}(phen)]^{2+}$ complex cations. Compound **5** features a mixed-valent As^{III}/As^V character and an interesting chalcogenidometalates structure, where a polycation formed by the connection of two $[Mn(2,2'\text{-bipy})_2]^{2+}$ complex cation and a $(As^VS_4)^{3-}$ anion acts as a countercation for a polythioarsenate anion, $[As^{III}S(S_5)]^-$. The title compounds exhibit optical gaps in the range 1.58−2.48 eV and blue photoluminescence. Interestingly, compound **1** displays a weak second harmonic generation (SHG) response being about 1/21 times of KTP ($KTiOPO_4$). Magnetic measurements show paramagnetic behavior for **1** and dominant antiferromagnetic behavior for **2**−**5**. Of particular interest is **4**, which is the first manganese chalcogenide showing spin-canting characteristic.

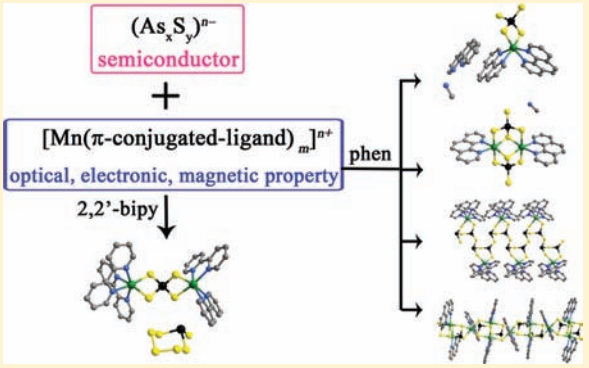

1. INTRODUCTION

Main-group element chalcogenide-based materials have garnered considerable attention arising not only from their fascinating structural features, but also as a result of their potential applications in nonlinear optics, ion exchange, photocatalysis, storage materials, electro-optics, and fast-ion conductivity.[1] Among these materials, those formed by the incorporation of unsaturated transition-metal (TM) or rare-earth-metal (Ln) complex cations into the inorganic main-group element chalcogenide frameworks have received much attention because of their unique topological structures and interesting physical properties.[1a,m,2] The very important aspect is that the optical and magnetic properties of the TM or Ln complexes may integrate with the unique properties of inorganic main-group element chalcogenide framework, which can be expected to give rise to complementary properties and synergistic effects.[2e,f] The mild hydro(solvo)thermal technique with in situ generated TM or Ln complex cations as templates or structure directors has been proved to be an effective method for the preparation of this type hybrid materials, which were usually performed in the presence of flexible aliphatic multidentate amine that not only acts as reaction medium but also as organic ligand chelating to TM or Ln ions.[1m,2f,3]

In comparison with traditional aliphatic chelating amines, chelating π-conjugated ligands featuring delocalized electrons over their aromatic rings can confer peculiar photochemical and electrochemical properties on their TM complex cations,[4] which may also have unusual structure directing abilities.[1p,5] It is very attractive to incorporate unsaturated TM π-conjugated ligand complex cations into inorganic main-group element chalcogenide frameworks to form hybrid chalcogenidometalates; however, studies on this area are limited,[6] especially, the physical property of the target compounds, which is usually not examined in detail. From a synthetic point of view, aliphatic multidentate chelating amines were usually used as an alkalinity regulator in the solvothermal syntheses of π-conjugated ligand-containing chalcogenidometalates;[6a,d−i] however, their alkalin-

Received: September 2, 2011
Published: December 8, 2011

   dx.doi.org/10.1021/ic201932z | Inorg. Chem. 2012, 51, 472−482

ity regulation ability is impeded by their strong chelating inclination to TM^{2+} ions, which will produce byproducts. Comparatively, monodentate organic amines with weaker monocoordinate ability with TM^{2+} ions can act as a well alkalinity regulator but were rarely used in the syntheses of π-conjugated ligand-containing chalcogenidometalates.[6b,c]

As a continuation of our work on the hydro(solvo)thermal syntheses of $[TM(\pi\text{-conjugated ligand})_m]^{n+}$ complex-containing chalcogenidometalates, phen (1,10-phenanthroline) and 2,2′-bipy (2,2′-bipyridine) ligands were used to yield a series of $[Mn(phen)_m]^{2+}$ (m = 1, 2) or $[Mn(2,2'\text{-bipy})]^{2+}$ fragment-containing thioarsenates with monodentate methylamine as an alkalinity regulator, namely, $(CH_3NH_3)\{[Mn(phen)_2](As^VS_4)\}\cdot$phen (**1** and **1′**), $(CH_3NH_3)_2\{[Mn(phen)]_2(As^VS_4)_2\}$ (**2**), $\{[Mn(phen)_2](As^{III}{}_2S_4)\}_n$ (**3**), $\{[Mn(phen)]_3(As^{III}S_3)_2\}\cdot H_2O$ (**4**), and $\{[Mn(2,2'\text{-bipy})_2]_2(As^VS_4)\}\cdot[As^{III}S(S_5)]$ (**5**). These compounds have diverse structures and show low-dimensional characteristics: zero-dimensional (0-D) for **1**−**2** and **5**, and one-dimensional (1-D) for **3**−**4**. Compound **1** comprises a $\{[Mn(phen)_2](As^VS_4)\}^-$ complex anion, a monoprotonated methylamine cation and a phen molecule, and represents the first example of main-group element chalcogenide with π-conjugated ligands exhibiting spontaneous resolution. Compound **2** contains a butterfly like $\{[Mn(phen)]_2(As^VS_4)_2\}^{2-}$ anion charge-compensated by two monoprotonated methylamine cations. Compound **3** represents the first example in which a helical $^1{}_\infty(As^{III}S_2^-)$ *vierer* chain covalently bonds to TM complexes via all its terminal S atoms. Compound **4** is a rare example, where the non-condensed $(As^{III}S_3)^{3-}$ anion is stabilized by coordinating to TM^{II} complex cations. Compound **5** features a mixed-valent As^{III}/As^V character and an interesting chalcogenidometalate structure, in which a polycation formed by the coordination of thioarsenate anion and unsaturated TM complex cation acts as a countercation for a polythioarsenate anion. Herein, we report the hydro(solvo)thermal syntheses, crystal structures, optical (SHG for **1**, UV−vis and photoluminescence) and magnetic properties of the five new manganese thioarsenates.

2. EXPERIMENTAL SECTION

2.1. Materials and Methods. All reagents were purchased commercially and used without further purification. Elemental analyses of C, H, and N were performed on an Elementar Vario EL III microanalyzer. Powder X-ray diffraction (PXRD) patterns were recorded on Rigaku MiniFlex II diffractometer using Cu Kα radiation. A NETZSCH STA 449C thermogravimetric analyzer was used to obtain TGA curves in N_2 with a flow rate of 20 mL/min and a ramp rate of 10 °C·min^{-1} in the temperature range 30−1000 °C. An empty Al_2O_3 crucible was used as the reference. The FT-IR spectra were obtained on a Perkin-Elmer spectrophotometer using KBr disk in the range 4000−400 cm^{-1}. The solid-state fluorescence emission spectra were measured on an Edinberg EI920 fluorescence spectrophotometer at room temperature with a wavelength increment of 1.0 nm and an integration time of 0.2 s. Optical diffuse reflectance spectra were measured at room temperature with a PE Lambda 900 UV−vis spectrophotometer. The instrument was equipped with an integrating sphere and controlled by a personal computer. The samples were ground into fine powder and pressed onto a thin glass slide holder. A $BaSO_4$ plate was used as a standard (100% reflectance). The absorption spectra were calculated from reflectance spectrum using the Kubelka−Munk function: $\alpha/S = (1 - R)^2/2R$[7] where α is the absorption coefficient, S is the scattering coefficient (which is practically wavelength independent when the particle size is larger than 5 μm), and R is the reflectance. The polycrystalline magnetic study was performed on a Quantum Design MPMS-XL SQUID or a PPMS-9T magnetometer. All data was corrected for diamagnetism estimated from Pascal's constants. Powder SHG measurement on the sample of **1** was performed on a modified Kurtz-NLO system using 1064 and 1905 nm laser radiation. The SHG signal was collected and focused into a fiber optic bundle. The output of the fiber optic bundle was coupled to the entrance slit of a spectrometer and detected using a CCD detector. KTP powder was used as a reference to assume the second-order NLO effect. SHG efficiency has been shown to depend strongly on particle size, thus the sample of KTP, as well as **1** were ground and sieved into the particle size in the range of 100−150 μm.

2.2. Syntheses. It should be mentioned that compounds **1**−**5** are gained in relatively low yields (8−17%) despite a broad variation of the synthesis conditions. The described synthesis methods below are the best ones to yield the title compounds up to now and the reproducibility of all the products are good. The synthetic conditions of **1**−**5** and related phases are summarized in Table 1. The crystals of the title compounds are stable in air and insoluble in common solvents and their phase purities are confirmed by PXRD studies (Figure S1, Supporting Information).

Table 1. Summary of the Synthetic Conditions of 1−5 and Related Phases

reactant	molar ratio of reactants	T [°C]	phase
As/$MnCl_2\cdot4H_2O$/S/phen·H_2O/H_2O/CH_3NH_2	0.51/0.5/3.5/1/17.85/162.35	150	**1**[a]
As/$MnCl_2\cdot4H_2O$/S/phen·H_2O/H_2O/CH_3NH_2	0.51/0.5/2/0.5/17.85/162.35	150	**2**[b]
As/$MnCO_3$/S/phen·H_2O/H_2O/CH_3NH_2	1/0.5/2/1/23.80/105.48	150	**3**
As/$MnCl_2\cdot4H_2O$/S/phen·H_2O/H_2O/CH_3NH_2	0.51/0.5/3.5/0.5/8.92/206.04	170	**4**
As/$MnCO_3$/S/2,2′-bipy/H_2O	0.51/0.5/2.5/1/278	150	**5**
As/$MnCl_2\cdot4H_2O$/S/phen·H_2O/H_2O/CH_3NH_2	0.5/0.5/2/0.5/23.80/105.48	150	**6**[6c]
As/$MnCO_3$/S/2,2′-bipy/H_2O	1/1/7/0.5/278	180	**7**[6a]
As/$MnCO_3$/S/2,2′-bipy/H_2O/dien	1/1/7/0.5/278/0.93	180	**8**[6a]

[a]The main product is **1**; the byproduct is **2**. [b]The main product is **2**; the byproduct is **1**. Phases **6**, **7**, and **8** has the formula of $\{[Mn(phen)]_3(As^VS_4)(As^{III}S_3)\}_n\cdot nH_2O$, $\{[Mn(2,2'\text{-bipy})]_3(As^VS_4)_2\}_n\cdot nH_2O$ and $\{[Mn(2,2'\text{-bipy})](MnAs^{III}{}_2S_5)\}$, respectively.

*2.2.1. Preparations of $(CH_3NH_3)\{[Mn(phen)_2](As^VS_4)\}\cdot$phen (**1** and **1′**) and $(CH_3NH_3)_2\{[Mn(phen)]_2(As^VS_4)_2\}$ (**2**).* A mixture of As (0.038 g, 0.51 mmol), $MnCl_2\cdot4H_2O$ (0.099 g, 0.50 mmol), S (0.112 g, 3.50 mmol), and phen·H_2O (0.198 g, 1.00 mmol) in 4.5 mL of methylamine aqueous solution (16% in H_2O) was sealed in a 25-mL poly(tetrafluoroethylene)-lined stainless steel container under autogenous pressure and then heated at 150 °C for 6 days and finally cooled to room temperature. Red prismatic crystals of **1** (Yield = 10% based on As) occurred together with red block crystals of **2** (Yield = 3% based on As) in the products. Attempts to obtain pure phase of **1** by changing reaction conditions such as temperature, the concentration of the methylamine aqueous solution, molar ratio of the starting materials, different metal sources (e.g., $MnCO_3$) as well as adding seed crystals in the starting materials were unsuccessful; compound **2** was always exist as byproduct in the products. Compound **2** could also be synthesized by the solvothermal reaction of As (0.038 g, 0.51 mmol), $MnCl_2\cdot4H_2O$ (0.099 g, 0.50 mmol), S (0.064 g, 2 mmol), and phen·H_2O (0.099 g, 0.50 mmol) in 4.5 mL of methylamine aqueous solution (16% in H_2O) for 5 days at 150 °C in a yield of 17% (based on As). Simultaneously, a small amount of crystals of **1** (yield = 2% based on As) was also observed in the products. Compounds **1** and **2**

dx.doi.org/10.1021/ic201932z | Inorg. Chem. 2012, 51, 472−482

Table 2. Crystal and Structure Refinement Data for 1−5

	1	1′	2
formula	$C_{37}H_{30}AsMnN_7S_4$	$C_{37}H_{30}AsMnN_7S_4$	$C_{26}H_{28}As_2Mn_2N_6S_8$
M_r (g mol^{-1})	830.78	830.78	940.74
cryst syst	orthorhombic	orthorhombic	monoclinic
space group	$P2_12_12_1$	$P2_12_12_1$	$P2_1/c$
Flack factor	0.022(8)	−0.003(5)	/
ρ_{calcd} [g cm^{-3}]	1.540	1.543	1.789
a [Å]	9.837(1)	9.832(1)	9.744(2)
b [Å]	14.443(1)	14.438(1)	20.901(3)
c [Å]	25.223(1)	25.197(1)	8.603(1)
α [deg]	90	90	90
β [deg]	90	90	94.682(11)
γ [deg]	90	90	90
V [Å^3]	3583.4(2)	3576.9(2)	1746.2(4)
Z	4	4	2
T [K]	293(2)	293(2)	293(2)
F(000)	1692	1692	940
θ range [deg]	2.82−25.50	2.51−25.50	1.95−25.48
measured reflns	29 315	23 420	3504
independent reflns (R_{int})	6654 (0.0459)	6645 (0.0418)	3255 (0.0325)
data/params/restraints	6469/452/0	6227/454/0	2538/202/0
$R_1{}^a$, $R_2{}^b$ [$I > 2\sigma(I)$]	0.0368, 0.0799	0.0238, 0.0490	0.0408, 0.0850
$R_1{}^a$, $R_2{}^b$ (all data)	0.0384, 0.0810	0.0260, 0.0498	0.0589, 0.0942
GOF	1.001	1.005	1.004
$\Delta\rho_{max}$ and $\Delta\rho_{min}$ [e Å^{-3}]	0.400, −0.406	0.357, −0.210	0.679, −0.489
	3	**4**	**5**
formula	$C_{24}H_{16}As_2MnN_4S_4$	$C_{36}H_{26}As_2Mn_3N_6OS_6$	$C_{40}H_{32}As_2Mn_2N_8S_{10}$
M_r (g mol^{-1})	693.43	1065.65	1205.06
cryst syst	monoclinic	monoclinic	triclinic
space group	$P2_1/c$	$P2_1/c$	$P\bar{1}$
Flack factor	/	/	/
ρ_{calcd} [g cm^{-3}]	1.810	1.794	1.648
a [Å]	13.369(1)	13.132(1)	12.954(2)
b [Å]	7.517(1)	20.239(1)	13.592(2)
c [Å]	25.358(2)	15.739(1)	15.011(2)
α [deg]	90	90	75.349(9)
β [deg]	93.278(4)	109.372(4)	86.827(9)
γ [deg]	90	90	71.791(10)
V [Å^3]	2544.3(3)	3946.1(5)	2428.2(5)
Z	4	4	2
T [K]	293(2)	293(2)	293(2)
F(000)	1372	2116	1208
θ range [deg]	2.83−25.50	2.01−25.50	1.63−25.49
measured reflns	16 522	28 270	9583
independent reflns (R_{int})	4708 (0.0213)	7328(0.0404)	9051 (0.0129)
data/params/restraints	4388/316/0	5208/493/21	6019/559/0
$R_1{}^a$, $R_2{}^b$ [$I > 2\sigma(I)$]	0.0262, 0.0525	0.0453, 0.1080	0.0420, 0.0833
$R_1{}^a$, $R_2{}^b$ (all data)	0.0287, 0.0538	0.0591, 0.1146	0.0842, 0.1011
GOF	0.992	1.005	1.006
$\Delta\rho_{max}$ and $\Delta\rho_{min}$ [e Å^{-3}]	1.040, −0.413	1.102, −0.850	0.729, −0.400

$^aR_1 = \sum||F_o| - |F_c||/\sum|F_o|$. $^bR_2 = \{\sum w[(F_o)^2 - (F_c)^2]^2/\sum w[(F_o)^2]^2\}^{1/2}$.

were manually separated and washed with ethanol and diethyl ether. Elemental analysis calcd. (%) for $C_{37}H_{30}AsMnN_7S_4$ (**1**): C 53.49, H 3.64, N 11.80; found C 53.61, H 3.50, N 11.82. Elemental analysis calcd. (%) for $C_{26}H_{28}As_2Mn_2N_6S_8$ (**2**): C 33.20, H 3.00, N 8.93; found C 33.30, H 2.82, N 8.89.

*2.2.2. Preparation of {[Mn(phen)$_2$](As$^{III}_2$S$_4$)}$_n$ (**3**).* A mixture of As (0.075 g, 1.00 mmol), $MnCO_3$ (0.058 g, 0.50 mmol), S (0.064 g, 2.00 mmol), and phen·H_2O (0.198 g, 1.00 mmol) in 4 mL of methylamine aqueous solution (28% in H_2O) was sealed in a 25-mL poly(tetrafluoroethylene)-lined stainless steel container under autogenous pressure and then heated at 150 °C for 6 days and finally cooled to room temperature. Dark-red prismatic crystals of **3** were selected by hand and washed with ethanol and diethyl ether. (yield = 13% based on As). Elemental analysis calcd. (%) for $C_{24}H_{16}As_2MnN_4S_4$: C 41.57, H 2.33, N 8.08; found C 41.46, H 2.14, N 8.10.

*2.2.3. Preparation of {[Mn(phen)]$_3$(As^{III}S$_3$)$_2$}·H$_2$O (**4**).* A mixture of As (0.038 g, 0.51 mmol), $MnCl_2·4H_2O$ (0.099 g, 0.50 mmol), S (0.112 g, 3.50 mmol), and phen·H_2O (0.099 g, 0.50 mmol) in 4.5 mL of methylamine aqueous solution (7% in H_2O) was sealed in a 25-mL poly(tetrafluoroethylene)-lined stainless steel container under autog-

dx.doi.org/10.1021/ic201932z | Inorg. Chem. 2012, 51, 472−482

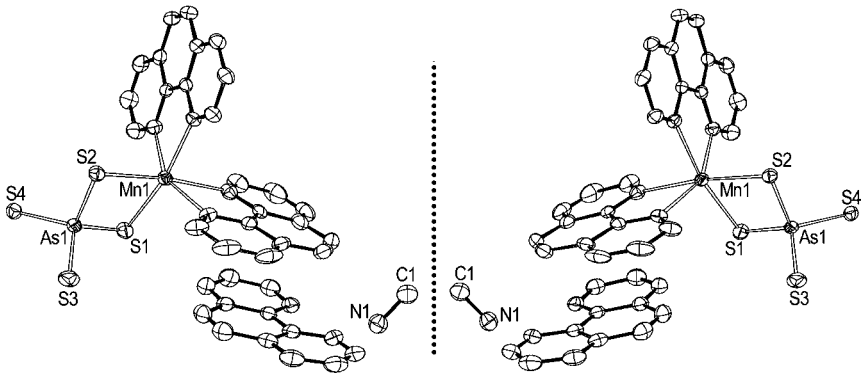

Figure 1. ORTEP drawing of **1** (left) and its mirror image **1′** (right) with 30% thermal ellipsoids and hydrogen atoms being omitted for clarity.

enous pressure and then heated at 170 °C for 6 days and finally cooled to room temperature. Black block crystals of **4** were selected by hand and washed with ethanol and diethyl ether (yield = 17% based on As). Elemental analysis calcd. (%) for $C_{36}H_{26}As_2Mn_3N_6OS_6$: C 40.58, H 2.46, N 7.89; found C 39.03, H 2.28, N 7.58.

*2.2.4. Preparation of {[Mn(2,2′-bipy)$_2$]$_2$(As^{V}S$_4$)}[As^{III}S(S$_5$)] (**5**).* A mixture of As (0.038 g, 0.51 mmol), $MnCO_3$ (0.058 g, 0.50 mmol), S (0.080 g, 2.50 mmol), and 2,2′-bipy (0.156 g, 1.00 mmol) in 5 mL of distilled water was sealed in a 25-mL poly(tetrafluoroethylene)-lined stainless steel container under autogenous pressure and then heated at 150 °C for 5 days and finally cooled to room temperature. Red block crystals of **5** were selected by hand and washed with ethanol and diethyl ether (yield = 8% based on As). Elemental analysis calcd. (%) for $C_{40}H_{32}As_2Mn_2N_8S_{10}$: C 39.87, H 2.68, N 9.30; found C 39.43, H 2.66, N 9.04.

2.3. Single-Crystal Structure Determination. Single crystals of **1**−**5** suitable for X-ray analyses were mounted at the apex of a glass fiber for data collection. Data collections were performed at 293(2) K on a Rigaku Saturn 724 CCD diffractometer for **1**, a Rigaku Mercury CCD diffractometer for **1′** and **3**, a Rigaku AFC7R diffractometer for **2** and **5**, and a Rigaku SCXmini CCD diffractometer for **4**, each diffractometers being equipped with a graphite-monochromated Mo Kα radiation (λ = 0.71073 Å). The intensity data sets were collected with the ω-scan technique for **1**, **1′**, **3**, and **4**, and ω−2θ scan technique for **2** and **5** and reduced by CrystalClear,[8] CrystalStructure[9] programs, respectively. Empirical absorption corrections, multiscan for **1**, **1′**, **3**, and **4**, and psi-scan for **2** and **5**, were applied. The structures were solved by direct methods using the Siemens SHELXL package of crystallographic software.[10] The difference Fourier maps created on the basis of these atomic positions to yield the other non-hydrogen atoms. The structure was refined using a full-matrix least-squares refinement on F^2. All non-hydrogen atoms were refined anisotropically. The hydrogen atoms of 2,2′-bipy, phen and methylamine molecules were added geometrically and refined as riding on their parent atoms with fixed isotropic displacement parameters [U_{iso}(H) = 1.2U_{eq}(C, N)]. The hydrogen atoms of lattice water molecules for **4** were located by different Fourier maps and refined with O−H distances to a target value of 0.85 Å and U_{iso}(H) = 1.5U_{eq}(O). Crystallographic data and structural refinements for the five compounds are summarized in Table 2.

3. RESULTS AND DISCUSSION

3.1. Synthesis Considerations. The mild hydro(solvo)-thermal reaction has been conducted to prepare the title compounds, in which the unsaturated TM π-conjugated ligand complexes are formed in situ and form covalent TM−S bonds with the thioarsenate anions. As we know, in a special hydro(solvo)thermal process, many factors can affect the formation and crystal growth of the product phases, such as initial reactants, reactant stoichiometry, pressure, pH value, temperature, reaction time, etc., and the successful preparation of a new compound is mainly the result of a systematic variation of the synthesis parameters. We have studied the influence of several synthetic parameters on the obtained compounds. Note that methylamine aqueous solution, acting as an organic base, offers the alkaline condition in the syntheses of **1**−**4**. The alkalinity data of the synthetic mixtures are summarized in Table S1 (Supporting Information). Compounds **1**−**3** are well isolated with the optimized concentration of the methylamine aqueous solution in the range of 16−28%; otherwise, the yields of **1**−**3** are lowed. Compound **4** can be obtained with the optimized concentration of the methylamine aqueous solution in the range 7−11%; otherwise, the expected crystal was not formed. Compound **5** is well isolated with distilled water used as solvent; further experiments with methylamine aqueous solution instead of distilled water are fruitless. The temperature does not play a decisive role in the formation of the five compounds, although it is directly related to the yields of the products. $MnCO_3$ used in the syntheses of **3** and **5** or $MnCl_2{\cdot}4H_2O$ used in the syntheses of **1**, **2** and **4** is perfect as the Mn^{2+} source material in our experiments. Detailed experiments show that compounds **1**−**5** still can be formed in a lower yield when the Mn^{2+} sources are replaced, that is, $MnCl_2{\cdot}4H_2O$ is replaced by $MnCO_3$ in the syntheses of **1**, **2**, and **4**, and $MnCO_3$ is replaced by $MnCl_2{\cdot}4H_2O$ in the syntheses of **3** and **5**.

3.2. Crystal Structures. In the title compounds, all thioarsenate anions, for example, tetrahedral $(AsS_4)^{3-}$ in **1**, **2**, and **5**, and pyramidal $(AsS_3)^{3-}$ in **3**−**4** exhibit As−S bond lengths and S−As−S bond angles demonstrating the distortion from their ideal geometries. The Mn^{2+} cations are all in octahedral coordination geometries and the bond lengths and angles clearly show their distortions from an ideal octahedron. The individual geometric parameters for these polyhedra are summarized in Table S2 (Supporting Information).

*3.2.1. Crystal Structures of Enantiomers **1** and **1′**.* Single-crystal X-ray diffraction analyses reveal that enantiomers **1** and **1′** crystallize in the same chiral space group $P2_12_12_1$ with Flack parameters of 0.022(8) and −0.003(5), respectively, indicating enantiomeric purity of the single crystals despite the use of achiral reagents. Here we only describe the detailed crystal structure of **1′**, which comprises a $\{[Mn(phen)_2](As^VS_4)\}^-$ complex anion, a monoprotonated methylamine cation and a phen molecule (Figure 1). The As1 atom is coordinated by four S atoms to form a $(As^VS_4)^{3-}$ tetrahedron. The Mn1 octahedron contains four N atoms from two chelating phen ligands and two S atoms from one chelating $(As^VS_4)^{3-}$ anion showing a Δ configuration. One $(As^VS_4)^{3-}$ tetrahedron connects with one

dx.doi.org/10.1021/ic201932z | Inorg. Chem. 2012, 51, 472−482

$[Mn(phen)_2]^{2+}$ to form a *cis*-$\{[Mn(phen)_2](As^VS_4)\}^-$ complex anion, which is very similar with our previously reported $\{[Mn(en)_2](As^VS_4)\}^-$ complex anion except that the en ligands are replaced by phen ligands in **1** and **1′**.[11] As expected, the average As−S_t (S_t = terminal S atom) bond distance of 2.145(1) Å is about 0.043 Å shorter than the average As−μ_2-S_b (S_b = bridging S atom) bond distances of 2.188(1) Å. As shown in Supporting Information Figure S2a, the monoprotonated methylamine bridges the $\{[Mn(en)_2](As^VS_4)\}^-$ complex anions and the phen molecules via C−H···S, N−H···S, and N−H···N hydrogen bonds to form a left-handed 1-D helical chain with a pitch of 9.832(1) Å extending along the [100] direction. These left-handed chains are stacked in a parallel manner in the [010] and [011] directions, and further stabilized by $\pi\cdots\pi$ stacking interactions to produce a homochiral three-dimensional (3-D) supramolecular structure (Supporting Information Figure S2b). It is interesting to mention that the structure of **1′** can also be described as a 3-D porous supramolecular host−guest architecture. The host framework is constructed by $\{[Mn(phen)]_2(As^VS_4)_2\}^-$ complex anions and discrete phen molecules through face-to-face $\pi\cdots\pi$ stacking interactions and the guest methylamine molecules reside in the parallelogram-like channels along the [100] direction interacting with the host framework via hydrogen bonds (Supporting Information Figure S2c and Table S3). In **1**, the molecule structure, the helical chain as well as the 3-D supramolecular structure all show opposite chiralities to those of **1′** (Supporting Information Figure S3).

Chirality is an essential feature of life, and also plays an important role in functional materials.[12] Chiral architectures can be obtained either by enantioselective synthesis using chiral species[13] or by spontaneous resolution using achiral species generating a conglomerate (racemic mixture of chiral crystals).[14] The generation of chiral compounds from achiral precursors is still a relatively scare phenomenon and cannot be predictable because the laws of physics determining the processes are not yet fully understood.[15] In this case, the entantiomers **1** and **1′** were obtained in the same crystallization, indicating that the spontaneous resolution occurs during the course of the crystallization. To the best of our knowledge, this is the first observation of main-group element chalcogenide with π-conjugated ligands exhibiting spontaneous resolution. It is well-known that homochiral assembly requires efficient transfer of stereochemical information between neighboring homochiral components. By inspection of the crystal structures of **1** and **1′**, it is believed that the chiral $\{[Mn(phen)_2](As^VS_4)\}^-$ complex anions are important for the formation of the chiral structures of **1** and **1′**, which can be understood in terms of chirality transfer from chiral complex anions to 1-D helical chains via hydrogen bonds and finally to whole framework through interchain $\pi\cdots\pi$ stacking interactions. This result demonstrates that chiral chalcogenidometalates can be constructed from achiral materials which are induced by π-conjugated ligand and main-group element chalcogenide anion simultaneously chelating to a TM cation. Because all starting materials are achiral, the bulk product is expected to be a 50:50 mixture of the two enantiomers.

3.2.2. Crystal Structure of **2**. Compound **2** contains a butterfly like $\{[Mn(phen)]_2(As^VS_4)_2\}^{2-}$ cluster and two charge-compensating monoprotonated methylamines cations (Figure 2). The $\{[Mn(phen)]_2(As^VS_4)_2\}^{2-}$ cluster is centrosymmetric and contains two symmetry-related $[Mn(phen)]^{2+}$ complexes bridged by two symmetry-related $(As^VS_4)^{3-}$ anions with a

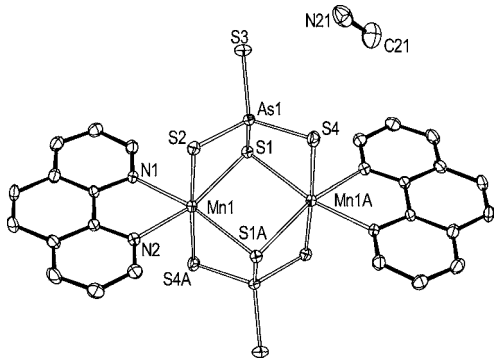

Figure 2. ORTEP drawing of **2** with 30% thermal ellipsoids and hydrogen atoms being omitted for clarity. Symmetry code: A ($1-x$, $1-y$, $1-z$).

(Mn_2S_2) four-membered ring and a Mn···Mn distance of 3.696(1) Å. Butterfly like cluster with the general formula $\{[TM(L)]_2(M'Q_4)_2\}^{q-}$ (L = bidentate chelating ligand; M′ = main-group element; Q = S, Se) can also be found in two 1-D thioarsenates $\{[Mn(2,2'\text{-bipy})]_3(As^VS_4)_2\}_n\cdot nH_2O$[6a] and $\{[Mn(phen)]_3(As^VS_4)_2\}_n\cdot nH_2O$,[6g] where the $\{[Mn(L)]_2(As^VS_4)_2\}^{2-}$ clusters serve as second building units (SBUs) connected by $[Mn(L)]^{2+}$ fragments to generate the final structures, and can be found in two group IV chalcogenide: a selenogermanate[16] with a discrete $\{[Cr(en)]_2(GeSe_4)_2\}^{2-}$ cluster and a 1-D thiostannate[6b] with $\{[Mn(phen)]_2(SnS_4)_2\}^{4-}$ clusters as SBUs being connected by $[Mn(phen)]^{2+}$ complexes. Meanwhile, the hybrid cluster in **2** is also closely related with the known inorganic $[Mn_2(As^VS_4)_4]^{8-}$ cluster,[17] in which two terminal $(As^VS_4)^{3-}$ anions are replaced by two phen ligands in **2** (Supporting Information Figure S5). Similar to **1** and **1′**, the methylamine molecules are monoprotonated for charge-balance requirement, which is confirmed by the IR spectrum as discussed in the Supporting Information. The As atom is coordinated by four S atoms to form a $(As^VS_4)^{3-}$ tetrahedron with three of its S atoms coordinating with two $[Mn(phen)]^{2+}$ fragments: two S atoms connecting two Mn^{2+} ions in a monodentate fashion, the third S atom forming a bridge between the Mn^{2+} ions. The As−S bond distances are normal and in the order of As−S_t < As−μ_2-S_b < As−μ_3-S_b (Supporting Information Table S2). In the crystal structure of **2**, the $\{[Mn(phen)]_2(As^VS_4)_2\}^{2-}$ clusters interact with the neighboring ones through face-to-face $\pi\cdots\pi$ stacking interactions between the aromatic rings of phen ligands chelating to Mn1 atoms to yield a 1-D chain-like structure along the [101] direction (Supporting Information Figure S6a). These chains are further stacked in parallel and stabilized by C−H···S hydrogen bonds to produce two-dimensional (2-D) layers parallel to the *ac* plane (Supporting Information Figure S6b, Table S4). Neighboring such layers are interconnected by monoprotonated methylamine molecules via N−H···S hydrogen bonds into a 3-D supramolecular framework of **2** (Supporting Information Figure S6c).

Taking into account that the butterfly like $\{[TM(L)]_2(M'Q_4)_2\}^{q-}$ clusters have been serve as SBUs in several novel hybrid main-group element chalcogenides, compound **2** may be used as a reaction precursor to synthesize new heterometallic thioarsenates.

3.2.3. Crystal Structure of **3**. The crystal structure of **3** consists of a neutral chiral chain $\{[Mn(phen)_2](As^{III}{}_2S_4)\}_n$, which can be regarded as unsaturated $[Mn(phen)_2]^{2+}$ complex

dx.doi.org/10.1021/ic201932z | *Inorg. Chem.* 2012, 51, 472−482

cations regularly bonding to the opposite side S atoms of the inorganic $^1_\infty(As^{III}S_2^-)$ anionic backbone chain. As shown in Figure 3, each Mn^{2+} ion in octahedral environment is

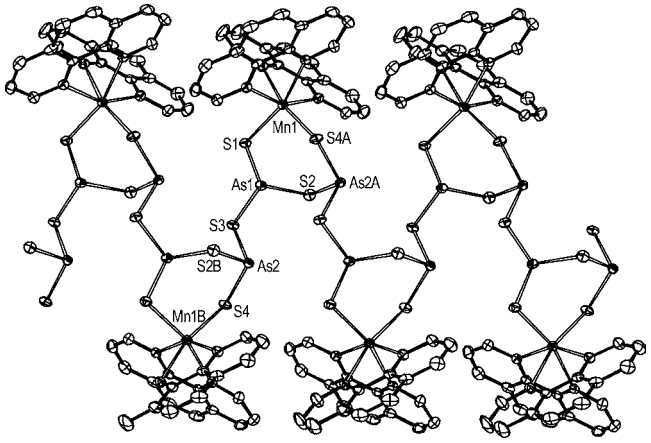

Figure 3. ORTEP view of a neutral chain $\{[Mn(phen)_2](As^{III}_2S_4)\}_n$ in **3** with 30% thermal ellipsoids. Hydrogen atoms are omitted for clarity. Symmetry codes: A $(1-x, 1/2+y, 1/2-z)$; B $(1-x, -1/2+y, 1/2-z)$.

coordinated by four N atoms of two phen ligands and two S atoms of the $^1_\infty(As^{III}S_2^-)$ chain. The As atom is coordinated by three S atoms to form a $(As^{III}S_3)^{3-}$ trigonal-pyramid, which is further self-condensed via sharing corners to produce helical $^1_\infty(As^{III}S_2^-)$ backbone chain. The single chain adopts *vierer* configuration,[18] containing four corner-sharing $(As^{III}S_3)^{3-}$ pyramids in the repeating unit with two kinds of As···As distances: 3.290(1) Å for As1···As2 and 3.391(1) Å for As1···As2A (A: 1−x, 1/2+y, 1/2−z). Each $(AsS_3)^{3-}$ in the $^1_\infty(As^{III}S_2^-)$ chain has two different S atoms: two μ_2-S_b atoms (bridging two As atoms) and one μ_2-S_b' atom (bridging the As and Mn atoms). The average As−μ_2-S_b bond distance of 2.290 Å is 0.096 Å longer than that of the average As−μ_2-S_b' bond distance of 2.194 Å (Supporting Information Table S2). There exist two opposite chiral $\{[Mn(phen)_2](As^{III}_2S_4)\}_n$ chains (left- and right-handed) in **3** (Supporting Information Figure S7). Adjacent homochiral chains are interconnected via interchain C−H···S hydrogen bonds to form homochiral 2-D layers parallel to the *ab* plane (Supporting Information Figures S8a and S8b). The layers with opposite chiralities are further packed alternately along the *c* direction and stabilized by interlayer C−H···S hydrogen bonds and face-to-face $\pi\cdots\pi$ stacking interactions leading to a 3-D achiral supramolecular structure of **3** (Supporting Information Figure S8c).

The 1-D structures with the general formula $^1_\infty(M^{III}Q_2^-)$ (M = As, Sb) formed by corner sharing $(M^{III}Q_3)^{3-}$ pyramids represent a typical family of 1-D main-group element chalcogenide anionic single chains. A number of $^1_\infty(M^{III}Q_2^-)$ single chains have been reported in group V chalcogenides,[1i,18,19] which show two different conformations, *zweier* and *vierer*; however, such chains showing helical character like that in **3** are very limited.[19l−o] Furthermore, compound **3** is also unique in that the helical $^1_\infty(As^{III}S_2^-)$ chain covalently bonds to TM complexes via all its terminal chalcogen atoms, which is different from the most related compound $\{[Mn(tren)](As_2Se_4)\}$,[19l] in which half of the terminal chalcogen atoms of the helical $^1_\infty(As^{III}Se_2^-)$ chain participate in the coordination with TM complex cations.

3.2.4. Crystal Structure of 4. Compound **4** is composed of neutral chains in stoichiometric $\{[Mn(phen)]_3(As^{III}S_3)_2\}_n$ and lattice water molecules. There are two crystallographically distinct As atoms in the asymmetric unit, each of which is coordinated by three S atoms to form a distorted $(As^{III}S_3)^{3-}$ pyramid (Figure 4). The Mn distorted octahedral configuration

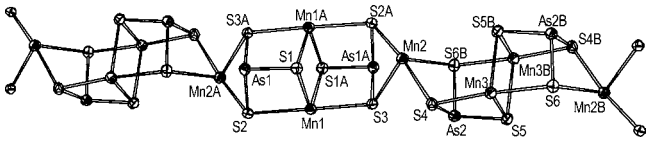

Figure 4. ORTEP view of a neutral chain $\{[Mn(phen)]_3(As^{III}S_3)_2\}_n$ in **4** with 30% thermal ellipsoids. The phen molecules are omitted for clarity. Symmetry codes: A $(2-x, 1-y, 1-z)$; B $(1-x, 1-y, -z)$.

involves four S atoms from two chelating $(As^{III}S_3)^{3-}$ pyramids and two N atoms from a phen ligand. Two neighboring symmetry-related $(As^{III}S_3)^{3-}$ pyramids are linked by two symmetry-related $[Mn(phen)]^{2+}$ complexes to form a centrosymmetric $\{[Mn(phen)]_2(As^{III}S_3)_2\}^{2-}$ cluster, which is further connected by $[Mn2(phen)]^{2+}$ fragments in a trans mode to yield a neutral chain extending along the [101] direction. Notably, unlike the $\{[Mn(phen)]_2(As^{V}S_4)_2\}^{2-}$ cluster in **2**, in which the As atoms have a valence of +5 and are in a tetrahedral coordination environment, the As atoms in the $\{[Mn(phen)]_2(As^{III}S_3)_2\}^{2-}$ cluster in **4** have a valence of +3 and locate in a trigonal-pyramidal coordination environment. The $\{[Mn(phen)]_2(As^{III}S_3)_2\}^{2-}$ cluster in **4** and the $\{[Mn(phen)]_2(As^{V}S_4)_2\}^{2-}$ cluster in **2** show different bond distances. The average $As^{III}-\mu_3$-S bond distance of $\{[Mn(phen)]_2(As^{III}S_3)_2\}^{2-}$ cluster is 2.256(1) Å, which is 0.053 Å longer than the $As^{V}-\mu_3$-S bond distance 2.203(1) Å of $\{[Mn(phen)]_2(As^{V}S_4)_2\}^{2-}$ cluster. The average Mn−μ_3-S bond distances of $\{[Mn(phen)]_2(As^{III}S_3)_2\}^{2-}$ cluster is 2.606 Å, while that of $\{[Mn(phen)]_2(As^{V}S_4)_2\}^{2-}$ cluster is 2.657 Å. The average Mn−N bond distance of $\{[Mn(phen)]_2(As^{III}S_3)_2\}^{2-}$ (av. 2.284(2) Å) is slightly longer than that of $\{[Mn(phen)]_2(As^{V}S_4)_2\}^{2-}$ cluster (av. 2.253(3) Å) (Supporting Information Table S2). It is worth mentioning that the three S atoms of each $(As^{III}S_3)^{3-}$ anions in the $\{[Mn(phen)]_3(As^{III}S_3)_2\}_n$ chain all acting as a μ_3-S ligands bridge two Mn atoms to produce two types of intrachain Mn···Mn interactions: the Mn−$(\mu_3$-S$)_2$−Mn (double S bridge) with a shorter Mn···Mn distances vary from 3.345(1) to 3.422(1) Å and the Mn−μ_3-S−Mn (single S bridge) with a longer Mn···Mn distances in the range 4.471(1)−4.719 Å, which are all significantly shorter than the shortest interchain Mn···Mn distances of 9.078(1) Å. This is significantly responsible for the interesting magnetic properties, as discussed in detail later. The interchain face-to-face $\pi\cdots\pi$ stacking interactions between the aromatic rings of phen ligands with centroid−centroid distance varying from 3.529(2) to 3.719(2) Å and dihedral angles in the range of 6.31(9)−13.00(9) ° lead to a 3-D supramolecular framework, where the lattice water molecules interact with the framework through O−H···S hydrogen bonds (Supporting Information Figure S9, Table S6).

The most interesting structural feature of **4** is the presence of noncondensed $(As^{III}S_3)^{3-}$ anions that are stabilized by coordinating to TM^{II} complex cations. The stabilization of noncondensed $(M^{III}Q_3)^{3-}$ species in the coordination of unsaturated TM complex cations is very desirable, because it may combine the optical and magnetic properties of the TM

dx.doi.org/10.1021/ic201932z | *Inorg. Chem.* 2012, 51, 472−482

complexes with the expected SHG property induced by asymmetric $(M^{III}Q_3)^{3-}$ species in a single compound.[6c] Although it remains a great challenge because the pyramidal $(M^{III}Q_3)^{3-}$ anions shows a characteristic self-condensation inclination to form polynuclear or 1-D anionic species under hydro(solvo)thermal conditions, several examples are still obtained under certain reaction condition, in which noncondensed $(M^{III}Q_3)^{3-}$ are stabilized by coordinating to TM complex cations with a high valent (≥3+) TM center[20] or simultaneously coordinating to metal ions and TM^{II} complex cations.[2d,21] Before this work, the stabilization of noncondensed $(M^{III}Q_3)^{3-}$ anions by coordinating to TM^{II} complex cations can only be found in a thioarsenate $\{[Mn(phen)]_3(As^VS_4)(As^{III}S_3)\}_n \cdot nH_2O$ reported recently by us,[6c] in which noncondensed $(As^{III}S_3)^{3-}$ and tetrahedral $(As^VS_4)^{3-}$ anions coexist. Compound **4** exhibits blue photoluminescence and interesting magnetic properties, however the SHG property is not observed because the dipole moment of the asymmetric $(As^{III}S_3)^{3-}$ anion cancel each other in the centrosymmetric structure of **4** (Supporting Information Figure S10).

3.2.5. Crystal Structure of 5. Compound **5** comprises a crystallographically independent polythioarsenate anion $[As^{III}S(S_5)]^-$ and a polycation $\{[Mn(2,2'\text{-bipy})_2]_2(As^VS_4)\}^+$ (Figure 5). The latter is establish by a $(As^VS_4)^{3-}$ anion bridging two $[Mn(2,2'\text{-bipy})_2]^{2+}$ fragments in a chelating mode. Each Mn atoms in the $\{[Mn(2,2'\text{-bipy})_2]_2(As^VS_4)\}^+$ cation with a distorted octahedral geometry is six coordinated by four N atoms from two phen molecules and two S atoms from one $(As^VS_4)^{3-}$ anion. The As atoms show different coordination environments: As1 is coordinated by four S atoms to form a $(As^VS_4)^{3-}$ tetrahedron, while As2 is coordinated by one S atom and one S_5 unit to form a $[As^{III}S(S_5)]^-$ anion, which is rarely reported in the literature[22] and belongs to the well-known group V chalcogenide anion family of $[M^{III}Q(Q_x)]^-$ ($x > 2$). In **5**, there exist intercation face-to-face $\pi\cdots\pi$ stacking interactions between the aromatic rings of phen molecules with centroid−centroid distance varying from 3.478(1) to 3.811(1) Å and dihedral angles in the range of 0.00(13)−2.16(9) °, which link the polycations $\{[Mn(2,2'\text{-bipy})_2]_2(As^VS_4)\}^+$ into a 2-D extended layer structure parallel to the (111) plane (Supporting Information Figure S11a). The polythioarsenate anions $[As^{III}S(S_5)]^-$ bridge the layers through C−H···S hydrogen bonds to form a 3-D supramolecular framework of **5** (Supporting Information Figure S11b, Table S7).

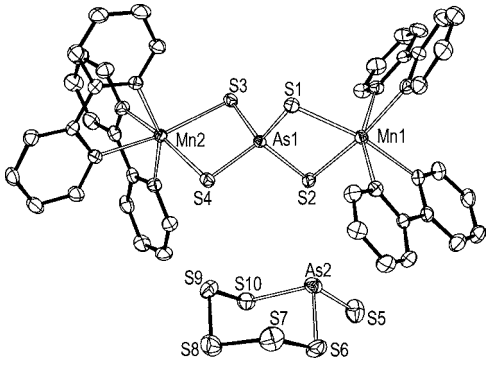

Figure 5. ORTEP drawing of **5** with 30% thermal ellipsoids and hydrogen atoms being omitted for clarity.

The main-group element chalcogenide-based compounds containing metal complex cations synthesized in the past years display intriguing crystal structures and have attracted substantial attention. In the vast majority of cases, the metal complex cations either act as template agents or structure directors discrete to the main-group element chalcogenide anions or covalently bond to main-group element chalcogenide anion forming neutral or negative-charged structures. Interestingly, the metal complex cations covalently bond to main-group element chalcogenide anions forming polycations are very limited.[23] So far the examples are only $[Mn(en)_3][\{[Mn(en)_2(H_2O)]_2(\mu\text{-}SbSe_4)\}[Mn(en)_2(\mu\text{-}SbSe_4)]Cl_2$,[23a] $\{[In(dien)]_2(InTe_4)\}Cl$,[23b] and $\{[In(C_6H_{14}N_2)_2]_2Sb_4S_8\}Cl_2$,[23c] in which the anions are the species formed by the connection of main-group element chalcogenide anion and TM complex cation, and/or halogen anions. Therefore, the most striking structural feature of **5** is its featuring an interesting structure type, where a polycation formed by the coordination of TM complex cation and thioarsenate anion acts as a countercation for a polythioarsenate anion. Similar feature is only found in a recently reported polyselenidoarsenates,[24] where a polycation $\{[Mn(phen)_2]_2(AsSe_4)\}^+$ acts as a countercation for a polythioarsenate anion $(As_2Se_6)^{2-}$.

For **5**, another interesting structural feature is its mixed-valent As^{III}/As^V character, which is in good agreement with the bond valence sum calculations As1 = 5.166, As2 = 2.885. The mixed-valent As^{III}/As^V character observed here, the +3 valent As in polythioarsenate $[As^{III}S(S_5)]^-$ anion, is quite different from several other chalcogenoarsenates,[6c,11,24,25] where the +3 valent As all exists in pyramidal $(As^{III}S_3)^{3-}$[5,6a−c] or in their self-condensed polymeric anionic species.[11,24,25]

3.2.6. Different Coordination Behaviors of the Unsaturated Mn^{II} phen or 2,2′-bipy Complexes in the Self-Assembly of 1−5. As typical bidentate chelating π-conjugated ligands, phen and 2,2′-bipy were used to form two types of unsaturated Mn π-conjugated ligand complex cations, $[Mn(\pi\text{-conjugated ligand})]^{2+}$ and $[Mn(\pi\text{-conjugated ligand})_2]^{2+}$, which exhibit different coordination behaviors when connecting with the inorganic thioarsenate anions in the self-assembly of **1**−**5**.

The unsaturated $[Mn(\pi\text{-conjugated ligand})]^{2+}$ complex cations featuring as many as four free coordination sites on a Mn center are prefer to be further coordinated by two chelating main-group element chalcogenide anions to achieve a 6-fold (MnN_2Q_4) coordination sphere as shown in **2** and **4**. In a few cases,[6c] the Mn center of $[Mn(\pi\text{-conjugated ligand})]^{2+}$ interact with main-group element chalcogenide anions via forming three Mn−Q bonds to adopt a 5-fold trigonal bipyramid coordination geometry. While, the $[Mn(\pi\text{-conjugated ligand})_2]^{2+}$ complex cation with two free coordination sites on the Mn center are prone to be further coordinated by a chelating main-group element chalcogenide anion,[6i] such as a discrete $(As^VS_4)^{3-}$ anion in **1** and **5**, and a $^1{}_\infty(As^{III}S_2^-)$ anion chain through two adjacent terminal S atoms in **3**.

Obviously, the different coordination behaviors of the $[Mn(\pi\text{-conjugated ligand})]^{2+}$ and $[Mn(\pi\text{-conjugated ligand})_2]^{2+}$ complex cations help to the formation of the title thioarsenates with diverse structures. Meanwhile, we note that similar unsaturated TM complex cations can direct different inorganic thioarsenate anions, such as the similar $[Mn(phen)_2]^{2+}$ cation direct tetrahedral $(AsS_4)^{4-}$ anion in **1** and 1-D $^1{}_\infty(As^{III}S_2^-)$ anionic chain in **3**, and the similar $[Mn(phen)_2]^{2+}$ cation direct $(AsS_4)^{4-}$ in **2** and noncondensed $(AsS_3)^{4-}$ in **4**, which suggests that besides TM complex cations as structure directors, the hydro(solvo)thermal synthetic

dx.doi.org/10.1021/ic201932z | Inorg. Chem. 2012, 51, 472−482

parameters also play an important role in determining the structures of the inorganic chalcogenide anionic network.[26]

3.3. Optical Spectroscopy and SHG Properties. Solid state UV−vis absorption spectra of **1**−**5** calculated from the diffuse reflectance data by using the Kubela−Mulk function are plotted in Figure 6.[27] The optical gaps (E_g) can be estimated as

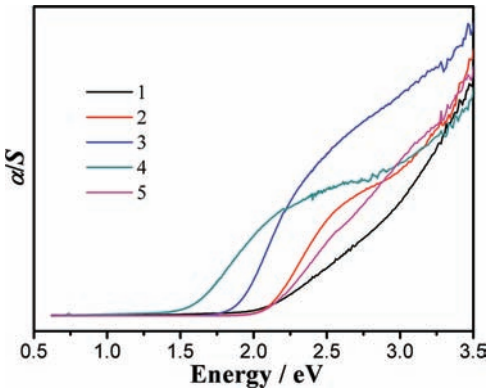

Figure 6. Optical diffuse reflectance spectra for **1**−**5**.

2.48 eV for **1**, 2.08 eV for **2**, 1.88 eV for **3**, 1.58 eV for **4**, and 2.12 eV for **5**, which are consistent with their color of the crystals, respectively.

Considering that compound **1** crystallizes in the acentric space group $P2_12_12_1$, it is worthy to study its SHG property. The sieved powder sample with the particle size in the range of 100−150 μm was first irradiated by 1064 nm laser light, but no green light was observed, which is ascribed to its absorption near the SHG wavelength (532 nm, Supporting Information Figure S16). However, when it was irradiated by 1905 nm laser light, a weak SHG response was observed, which is about 1/21 times that of KTP with the same particle size of 100−150 μm (KTP = $KTiOPO_4$, whose SHG response is more than 400 times that of quartz, Supporting Information Figure S17). On the basis of the structural data, the NLO behavior of **1** should originate from the cooperation of the polarizations of the polar units in **1**, including distorted (As^VS_4) and (MnN_4S_2) polyhedra, phen and methylamine molecules.

3.4. Magnetic Properties. Magnetic measurements were carried out on crystalline samples of **1**−**5**. According to the obtained data, there is paramagnetic behavior for **1** and antiferromagnetic behavior for **2**−**5**, in which, compound **4** exhibits interesting spin canting behavior. The magnetic properties of **1**−**3** and **5** are given in the Supporting Information. Some structural and magnetic data for **1**−**5** are listed in Table 3.

3.4.1. Magnetic Property of 4. The dc variable-temperature magnetic susceptibility of **4** was performed on crystalline sample in a field of 1000 Oe in the temperature range of 2−300 K. The plots of $\chi_M T$ versus T and χ_M versus T are shown in Figure 7a. The $\chi_M T$ value at 300 K is 10.477 $cm^3{\cdot}K{\cdot}mol^{-1}$, which is smaller than the spin-only value (13.125 $cm^3{\cdot}K{\cdot}mol^{-1}$) for three high-spin Mn^{2+} ions indicating the presence of strong antiferromagnetic interactions between Mn^{2+} ions even at high temperatures. The $\chi_M T$ value decreases continuously with decreasing temperature and reaches a minimum of 1.893 $cm^3{\cdot}K{\cdot}mol^{-1}$ at 8.4 K. On further cooling, $\chi_M T$ increases rapidly suggesting that a mechanism of ferromagnetic-like correlations exists. The $1/\chi_M$ versus T curve (Figure 7a, insert) above 100 K obeys the Curie−Weiss law with C = 21.26 emu·K/mol and θ = −311.4 K. The rather negative θ value indicates strong antiferromagnetic coupling among the Mn^{2+} ions. For an antiferromagnetic system, the ferromagnetic correlations can be attributed to spin canting, that is, perfect antiparallel alignment of the spins on neighboring metal ions within the antiferromagnetic chain is not achieved so that residual spins are generated.[28,29] To further characterize this phenomenon due to spin canting, field-cooled (FC) magnetizations at different fields were measured. As depicted in Figure 7b, the susceptibility below 9.3 K is rather field-dependent: the magnetization decreases with the increase of the applied field. This kind of field-dependence magnetic behavior confirms the weak ferromagnetism due to spin canting.[30] Further evidence comes from the isothermal field dependence of the magnetization M vs H at 2 K at fields up to 80 KOe (Figure 7c), which shows behavior typical of a canted antiferromagnet with a sharp increase of the magnetization at low fields and a linear variation of M at H > 20 KOe.[31] The magnetization value is 2.10 Nβ at 80 KOe, far from the saturation value of 15 Nβ for three Mn^{2+} ions (S = 5/2). Extrapolating the high-field linear part of the magnetization curve to zero field affords a magnetization value of 1.44 Nβ. Assuming this to be the uncompensated magnetization (M_{nc}), the spin canting angle α can be estimated to be about 16.07° by using the following simple relation, $\alpha = \tan^{-1}(M_{nc}/M_s)$,[28,32] where $M_s = gS\mu_B$ is the expected saturation magnetization if all of the moments are aligned ferromagnetically. Meanwhile, no significant magnetic hysteresis can be observed at 2 K, and the field cooled (FC) and zero-field-cooled (ZFC) susceptibility curves measured at 100 Oe are superposed at low temperatures (Figure S23). Moreover, both of in-phase (χ'_{ac}) and out-of-phase (χ''_{ac}) *ac* magnetic susceptibilities show no peaks down to 2 K. All these results indicate the absence of long-range magnetic ordering for **4** down to 2 K.

Although spin canting often provokes long-range magnetic ordering, as observed for some reported manganese com-

Table 3. Summary of the Magnetic Exchange Pathways, Minimum Mn···Mn Distances and Magnetic Parameters for 1−5

	1	2	3	4	5
bridging units		$(AsS_4)^{4-}$	$^1_\infty(AsS_2^-)$	$(AsS_3)^{4-}$	$(AsS_4)^{4-}$
possible magnetic exchange pathways	SMI[a]	$-\mu_3$-S−	−S−As−S−As−S−	$-\mu_3$-S−	−S−As−S−
∠Mn−S−Mn [deg]		88.15		80.74−127.30	
Mn···Mn [Å][b]		3.696	10.543	3.345−4.719	6.429
θ [K]	−0.9	−44.9	−4.3	−311.4	−6.0
J [cm^{-1}]		−3.27(4)	−0.15(1)		−0.56(1)
zJ' [cm^{-1}]		−0.95(5)	−0.14(2)		0.01(1)

[a]Supramolecular interaction. [b]Intrachain or intramolecular.

dx.doi.org/10.1021/ic201932z | Inorg. Chem. 2012, 51, 472−482

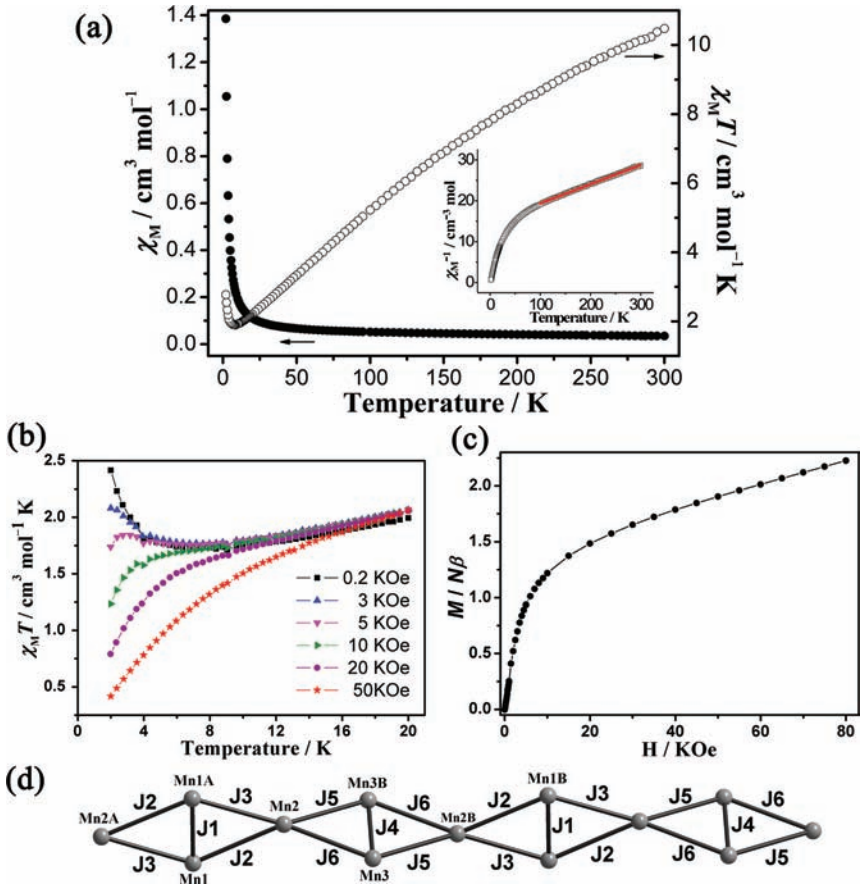

Figure 7. (a) Temperature dependence of χ_M and $\chi_M T$ for **4**. Insert: the temperature dependence of χ_M^{-1} for **4** with the solid line representing the fit of the Curie–Weiss law. (b) The $\chi_M T$ versus T curve below 20 K at different applied fields for **4**. (c) The field dependence isothermal magnetization for **4** at 2 K from 0 to 80 KOe. (d) The magnetic exchange pathways between adjacent Mn^{2+} ions.

pounds, however, which is not an obligatory consequence of spin-canting.[33] The examination of the structure suggests that the interchain magnetic interactions through supramolecular interactions (d(Mn···Mn) = 9.078(1) Å at a minimum) are significantly weaker than intrachain magnetic interactions via the μ_3-S atoms. Generally, the Mn^{2+} ions is considered to be a Heisenberg spin and therefore long-range magnetic order is only expected when magnetic exchange interactions propagate in all three dimensions through the structure.[34] In this case, the exchange between the chains is likely to be the limiting factor for long-range order and reflected on the absence of magnetic order down to 2 K. The possibility of the magnetic order taking place below 2 K was not investigated because of the measurements beyond the capability of our machine.

Take into consideration of the structural features of the compound, further inspection of the magnetic behaviors is worthwhile. Within the chain, the Mn^{2+} ions are all linked by the μ_3-S atoms with the Mn···Mn distances in the range of 3.345(1)–4.719(1) Å, which are still too long for significant direct magnetic exchange to occur, suggesting that coupling occurs via the μ_3-S atoms.[34b] According to the qualitative coupling rules,[35] all these superexchange interactions which are between high-spin d^5 Mn^{2+} ions via S atoms p-orbitals will be antiferromagnetic. However, the lack of an appropriate magnetic model to describe the magnetic system here has precluded quantitative magnetic analyses for **4**. Interestingly, three neighboring Mn^{2+} ions adopt a triangular arrangement in the chain (Figure 7d); as we know, a triangular arrangement of three spins with antiferromagnetic coupling can induce spin frustration. A parameter defined as $f = |\theta|/T_N$ that is widely used to measure the relative degree of the spin frustration, equals 155.7 at least (T_N < 2 K), indicating a strong frustration in the system.[36]

It is well-known that the occurrence of spin canting may arise from two mechanisms: (1) single-ion magnetic anisotropy and (2) the so-called antisymmetric Dzyaloshinsky–Moriya exchange coupling.[37] Because of the common isotropic character of the Mn^{2+} ion, the second factor should be responsible for the spin canting in **4**. It has been demonstrated that the antisymmetric exchange vanishes once an inversion center is present between neighboring spin centers.[37,38] In **4**, although the Mn^{2+} ions symmetrically linked by double μ_3-S atoms (Mn1–2(μ_3-S)–Mn1 and Mn3–2(μ_3-S)–Mn3) are related by inversion centers, there are no inversion centers between the Mn^{2+} centers linked via single μ_3-S atom (Mn1–μ_3-S–Mn2 and Mn2–μ_3-S–Mn3). It is expected that the antisymmetric exchange between the single μ_3-S atom bridged Mn^{II} centers is operative and superimposed upon the isotropic antiferromagnetic exchange, which is mainly responsible for the spin-canting phenomenon in **4**. The spin canting phenomenon of manganese(II) complexes have been well reported;[30b,31–33,34b,38] however, compound **4** represents, to the best of our knowledge, the first example in manganese chalcogenide materials.

3.4.2. Effects of the Bridging Thioarsenate Anions and Their Linkage Modes on the Magnetic Exchange Coupling.

dx.doi.org/10.1021/ic201932z | *Inorg. Chem.* 2012, 51, 472–482

The inorganic thioarsenate anions and their linkage modes with paramagnetic Mn^{2+} ions determine the magnetic exchange pathways in the title compounds, which finally influence the types and the strengths of the magnetic exchange coupling. In **2**−**5**, the thioarsenate anions bridge Mn^{2+} ions with the intramolecular (or intrachain) Mn···Mn distances in the range of 3.345−10.543 Å, which are far too long for significant direct magnetic exchanges (Figure 8, Table 3). Hence, the magnetic

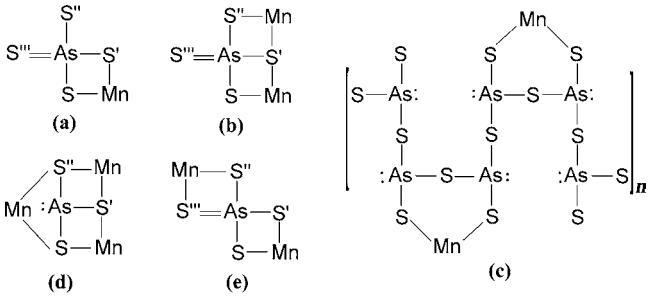

Figure 8. Linkage modes of the tetrahedral $(AsS_4)^{3-}$ anions in **1** (a), **2** (b), and **5** (e), the $^1_\infty(AsS_2^-)$ anionic chain in **3** (c) and the pyramidal $(AsS_3)^{3-}$ anion in **4** (d).

exchange is of superexchange type. Meanwhile, their superexchange pathways are closely related with the strengths of the magnetic couplings. The 1-D $^1_\infty(AsS_2^-)$ anionic chain in **3** and the $(AsS_4)^{4-}$ anion in **5** link the Mn^{2+} ions to generate weaker superexchange pathways, −S−As−S−As−S− and −S−As−S− (Figure 8c and 8e) with longer Mn···Mn distance of 10.543 and 6.429 Å, respectively, which finally lead to weaker antiferromagnetic couplings, $J = -0.15$ cm^{-1} and $\theta = -4.3$ K for **3** and $J = -0.56$ cm^{-1} and $\theta = -6.0$ K for **5**. In contrast, the tetrahedral $(AsS_4)^{4-}$ anions in **2**, and the pyramidal $(AsS_3)^{4-}$ anion in **4** chelating with the Mn^{2+} ions lead to a stronger superexchange pathway, $-\mu_3$-S−, (Figure 8b and 8d) with shorter Mn···Mn distances of 3.696 Å for **2** and 3.345−4.719 Å for **4**, which induce relatively stronger antiferromagnetic couplings (Table 3).

4. CONCLUSION

Our exploration in the hydro(solvo)thermal reaction systems As/S/Mn^{2+}/phen/methylamine aqueous solution and As/S/Mn^{2+}/2,2′-bipy/H_2O affords five new thioarsenates showing the existence of two different unsaturated Mn^{II} complex cations: the [Mn(π-conjugated ligand)]$^{2+}$ complexes in **2** and **4**, and the [Mn(π-conjugated ligand)$_2$]$^{2+}$ complexes in **1**, **3** and **5**. In comparison with the traditional aliphatic bidentate chelating amines, which show a strong inclination to form saturated Mn^{II} complexes, the phen and 2,2′-bipy ligands perform well in forming unsaturated Mn complexes in the present cases, suggesting that more main-group element chalcogenides incorporated with unsaturated Mn complexes can be expected by using the bidentate chelating π-conjugated ligand. Property studies show that compounds **1**−5 exhibits blue photoluminescence originated from the π-conjugated ligands and dominant antiferromagnetic coupling between the adjacent Mn^{II} centers in **2**−**5**, particularly compound **4** showing spin-canting characteristic; these results suggest that the incorporation of unsaturated TM π-conjugated ligand complexes into inorganic main-group element chalcogenide frameworks can enrich the physical properties of the main-group element-based chalcogenides, and materials with multiple properties, such as interesting optical, electronic and magnetic properties can be expected by using this strategy. Further studies are in progress in our laboratory.

■ ASSOCIATED CONTENT

Ⓢ Supporting Information

Crystallographic data (CIFs; CCDC reference numbers 819891 (**1**), 819892 (**1′**), 819893 (**2**), 819894 (**3**), 819895 (**4**) and 819896 (**5**)), additional structural figures, TGA curves, IR spectra, PXRD patterns, UV absorption spectra, the magnetic properties of **1**−**3** and **5**, and the ac susceptibility measurement as well as field dependence of magnetization for **4**. This materials is available free of charge via the Internet at http://pubs.acs.org.

■ AUTHOR INFORMATION

Corresponding Author

*E-mail: gcguo@fjirsm.ac.cn.

■ ACKNOWLEDGMENTS

We gratefully acknowledge financial support by the NSF of China (20701037, 90922035), 973 program (2011CBA00505), Key Project from the CAS (KJCX2.YW.M10) and the NSF of Fujian Province (2008I0026, 2008F3115).

■ REFERENCES

(1) (a) Drake, G. W.; Kolis, J. W. *Coord. Chem. Rev.* **1994**, *137*, 131. (b) Dehnen, S.; Melullis, M. *Coord. Chem. Rev.* **2007**, *251*, 1259. (c) Sheldrick, W. S.; Wachhold, M. *Coord. Chem. Rev.* **1998**, *176*, 211. (d) Yuan, M.; Mitzi, D. B. *Dalton Trans.* **2009**, 6078. (e) Yaghi, O. M.; Sun, Z.; Richardson, D. A.; Groy, T. L. *J. Am. Chem. Soc.* **1994**, *116*, 807. (f) Parise, J. B.; Tan, K. M. *Chem. Commun.* **1996**, 1687. (g) MacLachlan, M. J.; Coombs, N.; Ozin, G. A. *Nature* **1999**, *397*, 681. (h) Shah, A.; Torres, P.; Tscharner, R.; Wyrsch, N.; Keppner, H. *Science* **1999**, *285*, 692. (i) Bera, T. K.; Song, J.-H.; Freeman, A. J.; Jang, J. I.; Ketterson, J. B.; Kanatzidis, M. G. *Angew. Chem., Int. Ed.* **2008**, *47*, 7828. (j) Ding, N.; Kanatzidis, M. G. *Nat. Chem.* **2010**, *2*, 187. (k) Feng, M.-L.; Kong, D.-N.; Xie, Z.-L.; Huang, X.-Y. *Angew. Chem., Int. Ed.* **2008**, *47*, 8623. (l) Su, W.; Huang, X.; Li, J.; Fu, H. *J. Am. Chem. Soc.* **2002**, *124*, 12944. (m) Li, J.; Chen, Z.; Wang, R.-J.; Proserpio, D. M. *Coord. Chem. Rev.* **1999**, *190*−*192*, 707. (n) Bu, X.; Zheng, N.; Feng, P. *Chem.*−*Eur. J* **2004**, *10*, 3356. (o) Zheng, N.; Bu, X.; Vu, H.; Feng, P. *Angew. Chem., Int. Ed.* **2005**, *44*, 5299. (p) Zheng, N.; Lu, H.; Bu, X.; Feng, P. *J. Am. Chem. Soc.* **2006**, *128*, 4528.

(2) (a) Bensch, W.; Näther, C.; Schur, M. *Chem. Commun.* **1997**, 1773. (b) Rejai, Z.; Lühmann, H.; Näther, C.; Kremer, R. K.; Bensch, W. *Inorg. Chem.* **2010**, *49*, 1651. (c) Manos, M. J.; Kanatzidis, M. G. *Inorg. Chem.* **2009**, *48*, 4658. (d) Wang, Z.; Zhang, H.; Wang, C. *Inorg. Chem.* **2009**, *48*, 8180. (e) Zhang, Q.; Bu, X.; Lin, Z.; Biasini, M.; Beyermann, W. P.; Feng, P. *Inorg. Chem.* **2007**, *46*, 7262. (f) Zhou, J.; Dai, J.; Bian, G.-Q.; Li, C.-Y. *Coord. Chem. Rev.* **2009**, *253*, 1221. (g) Zhou, J.; Bian, G.-Q.; Dai, J.; Zhang, Y.; Tang, A.-B.; Zhu, Q.-Y. *Inorg. Chem.* **2007**, *46*, 1541. (h) Chen, J.-F.; Jin, Q.-Y.; Pan, Y.-L.; Zhang, Y.; Jia, D.-X. *Chem. Commun.* **2009**, 7212.

(3) (a) Rabenau, A. *Angew. Chem., Int. Ed.* **1985**, *24*, 1026. (b) Sheldrick, W. S.; Wachhold, M. *Angew. Chem., Int. Ed.* **1997**, *36*, 207.

(4) (a) Konig, E. *Coord. Chem. Rev.* **1968**, *3*, 471. (b) Scaltrito, D. V.; Thompson, D. W.; O'Callaghan, J. A.; Meyer, G. J. *Coord. Chem. Rev.* **2000**, *208*, 243. (c) Polo, A. S.; Itokazu, M. K.; Iha, N. Y. M. *Coord. Chem. Rev.* **2004**, *248*, 1343. (d) Youngblood, W. J.; Lee, S. H. A.; Maeda, K.; Mallouk, T. E. *Acc. Chem. Res.* **2009**, *42*, 1966. (e) Kim, J. J.; Choi, H.; Kim, C.; Kang, M. S.; Kang, H. S.; Ko, J. *Chem. Mater.* **2009**, *21*, 5719. (f) Juris, A.; Balzani, V.; Barigelletti, F.; Campagna, S.; Belser, P.; Vonzelewsky, A. *Coord. Chem. Rev.* **1988**, *84*, 85. (g) Armaroli, N. *Chem. Soc. Rev.* **2001**, *30*, 113. (h) Lavie-Cambot,

A.; Cantuel, M.; Leydet, Y.; Jonusauskas, G.; Bassani, D. M.; McClenaghan, N. D. *Coord. Chem. Rev.* **2008**, *252*, 2572.
(5) (a) Lei, Z.-X.; Zhu, Q.-Y.; Zhang, X.; Luo, W.; Mu, W.-Q.; Dai, J. *Inorg. Chem.* **2010**, *49*, 4385. (b) Zhao, J.; Liang, J.; Chen, J.; Pan, Y.; Zhang, Y.; Jia, D. *Inorg. Chem.* **2011**, *50*, 2288.
(6) (a) Fu, M.-L.; Guo, G.-C.; Liu, X.; Chen, W.-T.; Liu, B.; Huang, J.-S. *Inorg. Chem.* **2006**, *45*, 5793. (b) Liu, G.-N.; Guo, G.-C.; Chen, F.; Guo, S.-P.; Jiang, X.-M.; Yang, C.; Wang, M.-S.; Wu, M. F.; Huang, J.-S. *CrystEngComm* **2010**, *12*, 4035. (c) Liu, G.-N.; Jiang, X.-M.; Wu, M.-F.; Wang, G.-E.; Guo, G.-C.; Huang, J.-S. *Inorg. Chem.* **2011**, *50*, 5740. (d) Kromm, A.; Sheldrick, W. S. *Z. Anorg. Allg. Chem.* **2008**, *634*, 1005. (e) Kromm, A.; Sheldrick, W. S. *Z. Anorg. Allg. Chem.* **2008**, *634*, 2948. (f) Kromm, A.; Sheldrick, W. S. *Z. Anorg. Allg. Chem.* **2009**, *635*, 205. (g) Wang, X.; Sheng, T.-L.; Hu, S.-M.; Fu, R.-B.; Chen, J.-S.; Wu, X.-T. *J. Solid State Chem.* **2009**, *182*, 913. (h) Wang, X.; Sheng, T.-L.; Hu, S.-M.; Fu, R.-B.; Wu, X.-T. *Inorg. Chem. Commun.* **2009**, *12*, 399. (i) Pan, Y.; Jin, Q.; Chen, J.; Zhang, Y.; Jia, D. *Inorg. Chem.* **2009**, *48*, 5412.
(7) Wendlandt, W. M.; Hecht, H. G. *Reflectance Spectroscopy*; Interscience: New York, 1966.
(8) *CrystalClear*, version 1.35; Rigaku Corp.: Tokyo, Japan, 2002.
(9) *CrystalStructure*, version 3.10; Rigaku Corp. and Rigaku/MSC: Tokyo, Japan, 2002.
(10) *SHELXTL Reference manual*, version 5; Siemens Energy & Automaion Inc.: Madision,WI, 1994.
(11) Fu, M.-L.; Guo, G.-C.; Cai, L.-Z.; Zhang, Z.-J.; Huang, J.-S. *Inorg. Chem.* **2005**, *44*, 184.
(12) (a) Collins, A. N., Sheldrake, G. N., Crosby, J., Eds.; *Chiral in Industry II*.Wiley: New York, 1998. (b) Lin, W. *MRS Bull.* **2007**, *32*, 544. (c) Zhang, J.; Chen, S.; Zingiryan, A.; Bu, X. *J. Am. Chem. Soc.* **2008**, *130*, 17246.
(13) Knof, U.; von Zelewsky, A. *Angew. Chem., Int. Ed.* **1999**, *38*, 302.
(14) Pérez-García, L.; Amabilino, D. B. *Chem. Soc. Rev.* **2002**, *31*, 342.
(15) Gao, E.-Q.; Bai, S.-Q.; Wang, Z.-M.; Yan, C.-H. *J. Am. Chem. Soc.* **2003**, *125*, 4984.
(16) Melullis, M.; Brandmayer, M. K.; Dehnen, S. *Z. Anorg. Allg. Chem.* **2006**, *632*, 64.
(17) Iyer, R. G.; Kanatzidis, M. G. *Inorg. Chem.* **2004**, *43*, 3656.
(18) Bera, T. K.; Jang, J. I.; Song, J. H.; Malliakas, C. D.; Freeman, A. J.; Ketterson, J. B.; Kanatzidis, M. G. *J. Am. Chem. Soc.* **2010**, *132*, 3484.
(19) (a) Konig, T.; Eisenmann, B.; Schafer, H. *Z. Anorg. Allg. Chem.* **1982**, *488*, 126. (b) Stahler, R.; Bensch, W. *Eur. J. Inorg. Chem.* **2001**, 3073. (c) Schaefer, M.; Kurowski, D.; Pfitzner, A.; Näther, C.; Rejai, Z.; Möller, K.; Ziegler, N.; Bensch, W. *Inorg. Chem.* **2006**, *45*, 3726. (d) Stephan, H. O.; Kanatzidis, M. G. *Inorg. Chem.* **1997**, *36*, 6050. (e) Stephan, H. O.; Kanatzidis, M. G. *J. Am. Chem. Soc.* **1996**, *118*, 12226. (f) Jia, D.-X.; Zhang, Y.; Dai, J.; Zhu, Q.-Y.; Gu, X.-M. *J. Solid State Chem.* **2004**, *177*, 2477. (g) Lees, R. J. E.; Powell, A. V.; Chippindale, A. M. *Polyhedron* **2005**, *24*, 1941. (h) Palazzi, M.; Jaulmes, S. *Acta Crystallogr. B* **1977**, *33*, 908. (i) Yang, Z. M.; Pertlik, F. *J. Alloys Compd.* **1994**, *216*, 155. (j) Eisenmann, B.; Schafer, H. *Z. Anorg. Allg. Chem.* **1979**, *456*, 87. (k) Sheldrick, W. S.; Hausler, H. J. *Z. Anorg. Allg. Chem.* **1988**, *561*, 139. (l) Kromm, A.; Sheldrick, W. S. *Z. Anorg. Allg. Chem.* **2008**, *634*, 225. (m) Fleet, M. E. *Z. Kristallogr.* **1973**, *138*, 147. (n) Smith, J. V.; Pluth, J. J.; Han, S. X. *Mineral. Mag.* **1997**, *61*, 671. (o) Effenberger, H.; Paar, W. H.; Topa, D.; Criddle, A. J.; Fleck, M. *Am. Mineral.* **2002**, *87*, 753. (p) Dovgoshe, Ni; Nikolyuk, V. I.; Semrad, E. E.; Chepur, D. V.; Golovei, M. I. *Izv. Vyssh. Uchebn. Zaved., Fiz.* **1970**, 138. (q) Lada, A. V.; Zuban, V. A.; Borets, A. N.; Golovei, M. I. *Opt. Spektrosk.* **1974**, *37*, 582. (r) Bazakutsa, V. A.; Gnidash, N. I.; Perekrestov, V. I.; Lazarev, V. B.; Salov, A. V.; Trippel, A. F. *Inorg. Mater.* **1987**, *23*, 1020. (s) Kanishcheva, A. S.; Mikhailov, I. N.; Kuznetsov, V. G.; Batog, V. N. *Dokl. Akad. Nauk USSR* **1980**, *251*, 603.
(20) (a) Zank, G. A.; Rauchfuss, T. B.; Wilson, S. R.; Rheingold, A. L. *J. Am. Chem. Soc.* **1984**, *106*, 7621. (b) Schur, M.; Rijnberk, H.; Näther, C.; Bensch, W. *Polyhedron* **1999**, *18*, 101. (c) Vaqueiro, P.; Chippindale, A. M.; Powell, A. V. *Polyhedron* **2003**, *22*, 2839. (d) Möller, K.; Näther, C.; Bannwarth, A.; Bensch, W. *Z. Anorg. Allg. Chem.* **2007**, *633*, 2635.
(21) (a) Schaefer, M.; Näther, C.; Bensch, W. *Solid State Sci.* **2003**, *5*, 1135. (b) Kiebach, R.; Bensch, W.; Hoffmann, R. D.; Pöttgen, R. *Z. Anorg. Allg. Chem.* **2003**, *629*, 532. (c) Lichte, J.; Lühmann, H.; Näther, C.; Bensch, W. *Z. Anorg. Allg. Chem.* **2009**, *635*, 2021.
(22) Siewert, B.; Muller, U. *Z. Anorg. Allg. Chem.* **1992**, *609*, 82.
(23) (a) van Almsick, T.; Sheldrick, W. S. *Z. Anorg. Allg. Chem.* **2006**, *632*, 1413. (b) Li, C.-Y.; Chen, X.-X.; Zhou, J.; Zhu, Q.-Y.; Lei, Z.-X.; Zhang, Y.; Dai, J. *Inorg. Chem.* **2008**, *47*, 8586. (c) Quiroga-Gonzalez, E.; Näther, C.; Bensch, W. *Solid State Sci.* **2010**, *12*, 1235.
(24) Jia, D.; Zhao, J.; Pan, Y.; Tang, W.; Wu, B.; Zhang, Y. *Inorg. Chem.* **2011**, DOI: 10.1021/ic2007809..
(25) Kanatzidis, M. G.; Chou, J.-H. *J. Solid State Chem.* **1996**, *127*, 186.
(26) Seidlhofer, B.; Pienack, N.; Bensch, W. *Z. Naturforsch.* **2010**, *65b*, 937.
(27) The enantiomers **1** and **1′** were not separated because they have the same morphology, and the physical measurements were made on the mixture of them.
(28) Kahn, O. *Molecular Magnetism*; VCH: New York, 1993.
(29) Miller, J. S. *Adv. Mater.* **2002**, *14*, 1105.
(30) (a) Carlin, R. L. *Magnetochemistry*; Springer-Verlag: Berlin, 1986. (b) Ma, B.-Q.; Sun, H.-L.; Gao, S.; Su, G. *Chem. Mater.* **2001**, *13*, 1946.
(31) (a) Gao, E.-Q.; Yue, Y.-F.; Bai, S.-Q.; He, Z.; Yan, C.-H. *J. Am. Chem. Soc.* **2004**, *126*, 1419. (b) Riou-Cavellec, M.; Lesaint, C.; Nogues, M.; Greneche, J. M.; Ferey, G. *Inorg. Chem.* **2003**, *42*, 5669. (c) Mahata, P.; Sen, D.; Natarajan, S. *Chem. Commun.* **2008**, 1278.
(32) (a) Palacio, F.; Andres, M.; Horne, R.; Vanduyneveldt, A. J. *J. Magn. Magn. Mater.* **1986**, *54*−*57*, 1487. (b) Gavrilenko, K. S.; Punin, S. V.; Cador, O.; Golhen, S.; Ouahab, L.; Pavlishchuk, V. V. *J. Am. Chem. Soc.* **2005**, *127*, 12246.
(33) Gao, E.-Q.; Cheng, A.-L.; Xu, Y.-X.; He, M.-Y.; Yan, C.-H. *Inorg. Chem.* **2005**, *44*, 8822.
(34) (a) Mermin, N. D.; Wagner, H. *Phys. Rev. Lett.* **1966**, *17*, 1133. (b) Yang, M.; Yu, J.; Shi, L.; Chen, P.; Li, G.; Chen, Y.; Xu, R. *Chem. Mater.* **2006**, *18*, 476.
(35) Goodenough, J. B. *Magnetism and the Chemical Bond*; Wiley: New York, 1963.
(36) (a) Ramirez, A. P. *Annu. Rev. Mater. Sci.* **1994**, *24*, 453. (b) Greedan, J. E. *J. Mater. Chem.* **2001**, *11*, 37. (c) Wang, X. Y.; Sevov, S. C. *Chem. Mater.* **2007**, *19*, 3763.
(37) (a) Dzyaloshinsky, I. *J. Phys. Chem. Solids* **1958**, *4*, 241. (b) Moriya, T. *Phys. Rev.* **1960**, *120*, 91.
(38) (a) Armentano, D.; De Munno, G.; Lloret, F.; Palii, A. V.; Julve, M. *Inorg. Chem.* **2002**, *41*, 2007. (b) Gao, E.-Q.; Yue, Y.-F.; Bai, S.-Q.; He, Z.; Zhang, S.-W.; Yan, C.-H. *Chem. Mater.* **2004**, *16*, 1590.